Generalization of cylindrical spheromak solution to finite beta and large reversed shear

P. M. Bellan[a)]
128-95 Caltech, Pasadena, California 91125

(Received 19 February 2002; accepted 8 April 2002)

The well-known analytic solution for a spheromak in a cylindrical flux conserver is generalized to the situation of finite β with the shape of the flux conserver now being a dependent quantity. Analytic expressions are found for the poloidal flux surfaces, beta, the safety factors at both the magnetic axis and the wall, and the wall profile. A large reversed shear (i.e., ratio of safety factor on magnetic axis to safety factor at the wall) can be obtained at finite beta. This feature may be important because reversed shear in the core of tokamaks has been shown to permit stable operation at high β. © *2002 American Institute of Physics.* [DOI: 10.1063/1.1482071]

I. INTRODUCTION

Spheromaks are magnetohydrodynamic equilibria having closed field lines in a simply connected geometry.[1–5] They are an attractive configuration for a magnetic fusion reactor because they dispense with the cumbersome toroidal field coils and the doubly connected topology common to tokamaks, stellarators, and reversed field pinches. This simplicity of design offers the possibility of a less expensive and more compact reactor. Spheromak physics is also relevant to solar and astrophysical plasmas and, in particular, spheromak-like equilibria have been proposed for the solar corona[6] and also as the ejecta of the accretion disks[7] found in diverse astrophysical situations. Extensive modeling of spheromaks has been done using the assumption of zero hydrodynamic pressure compared to magnetic pressure (i.e., zero β).

In particular, it has been shown that a $\beta=0$ isolated plasma inside a simply-connected conducting boundary relaxes via magnetohydrodynamic (MHD) instabilities to a force-free state $\nabla\times\mathbf{B}=\lambda\mathbf{B}$, where λ is a spatially uniform eigenvalue.[3] The relaxation process assumes conservation of magnetic helicity and involves having λ gradients destabilize nonaxisymmetric current-driven instabilities that convect magnetic helicity across field lines; this helicity transport process tends to reduce the λ gradient and the relaxed state equilibrium is achieved when λ becomes spatially uniform (if the model is extended to include the much slower process of helicity dissipation, then some amount of λ gradient is required in steady state to allow for a continuous replenishment of the helicity; here we will restrict attention to the time scale on which helicity is conserved and so will not consider λ gradients, i.e., we assume that there is no free energy for current-driven instabilities). Since the relaxed state represents a situation where there is no longer free energy for current-driven instabilities, the remaining possibility for instability is pressure-driven instability, i.e., instabilities associated with finite β.

A commonly used force-free spheromak equilibrium is the so-called Bessel-function model (also called the Chandrasekhar–Kendall model) which is based on the assumptions that the configuration is symmetric about the z axis and is enclosed by a perfectly conducting cylindrical shell having radius a and height h.[5,8,9] The purpose of this paper is to generalize the $\beta=0$ Bessel function solution to finite β situations and to make a preliminary consideration of the ramifications of finite β. We note that finite β spheromak equilibria have been calculated previously,[10–13] but these equilibria were not generalizations of the cylindrical Bessel function solution.

II. REVIEW OF THE STANDARD CYLINDRICAL SPHEROMAK

The standard cylindrical spheromak has a magnetic field,

$$\mathbf{B}=\frac{1}{2\pi}(\nabla\psi\times\nabla\phi+\mu_0\lambda\psi\nabla\phi), \tag{1}$$

where the poloidal flux function is

$$\psi(r,z)=\psi_0\frac{rJ_1(\gamma r)}{r_0J_1(\gamma r_0)}\cos kz. \tag{2}$$

The magnetic axis is located at $r=r_0$, $z=0$ and is where ψ attains its maximum value, ψ_0. The axial wave number is quantized to be $k=\pi/h$ so that ψ vanishes at the top and bottom of the cylinder, i.e., at $z=\pm h/2$. The requirement that ψ vanishes at the cylinder wall $r=a$ constrains the eigenvalue γ to be such that $\gamma a=x_{11}$, where $x_{11}=3.832$ is the first zero of J_1. The location of the magnetic axis is determined by the requirement that ψ_0 is the maximum value of ψ and this condition gives $\gamma r_0=x_{01}$, where $x_{01}=2.405$ is the first zero of J_0. The eigenvalue γ is related to λ and k by $\gamma^2=\lambda^2-k^2$. In order to avoid tilt instability the height h is constrained to satisfy $h<1.8a$.[14,15]

This force-free solution has been used previously as a proxy to study the stability of finite β spheromaks with respect to interchange modes. Because the magnetic shear of force-free relaxed states is very low, these studies imply that spheromaks should not be able to support a β exceeding less

a)Electronic mail: pbellan@its.caltech.edu

than 0.01 on the presumption that the force-free solution is indeed a good approximation to the finite β equilibrium. However, experiments demonstrate[16] that spheromaks can support β as high as 0.2 without interchange instability; this discrepancy with the theoretical predictions casts doubt on the validity of using the results of a $\beta=0$ equilibrium to calculate the stability properties of a finite β equilibrium.

III. REQUIRED PROPERTIES FOR A FINITE β SPHEROMAK

The spheromak is assumed to be axisymmetric so that its equilibrium is governed by the Grad–Shafranov equation,[17,18]

$$r\frac{\partial}{\partial r}\left(\frac{1}{r}\frac{\partial\psi}{\partial r}\right)+\frac{\partial^2\psi}{\partial z^2}+4\pi^2\mu_0 r^2\frac{\partial P}{\partial\psi}+\mu_0 I\frac{\partial}{\partial\psi}(\mu_0 I)=0. \quad (3)$$

In order to be relevant to a spheromak the solution to Eq. (3) must have the following properties:

(1) The poloidal flux $\psi(r,z)$ must vanish both at $r=0$ and on some outer boundary. Unlike the cylindrical model, we will not specify the profile of the outer boundary, but instead will let this profile be part of the solution. We are interested in solutions that are symmetric in z. Regularity at $r=0$ requires the poloidal flux to be a function of r^2 for an azimuthally symmetric function.[19]

(2) The pressure is non-negative and since $P=P(\psi)$, the pressure must be of the form $P=P_0+\kappa_1\psi+\kappa_2\psi^2+\cdots$, where P_0 and the coefficients $\kappa_1,\kappa_2,\ldots$ are constants.

(3) Since $I=I(\psi)$, the current can be expressed as $\mu_0 I=\lambda_1\psi+\lambda_2\psi^2+\cdots$, where the coefficients $\lambda_1,\lambda_2,\ldots$ are constants. There is no constant term in this expansion so that I and hence the toroidal field vanish at the wall (this feature is what allows the spheromak to be simply connected and is in contrast to tokamaks or reversed field pinches which do have a constant term and which are not simply connected).

(4) There must be a local maximum in the poloidal flux in order to have a magnetic axis. We define ψ_0 to be the value of the poloidal flux at the magnetic axis, i.e., the maximum value of the poloidal flux.

IV. DERIVATION OF THE FINITE β SOLUTION

We now assume the simplest nontrivial pressure and current functional dependence that have the properties listed above, i.e., we assume

$$P=P_0\psi/\psi_0,\qquad \mu_0 I=\lambda\psi, \quad (4)$$

and seek a solution for ψ.

In order to proceed, we first make the following set of definitions and prescriptions:

(1) The pressure vanishes on the flux surface where $\psi=0$; this is the boundary of the spheromak.

(2) We define the radius r_0 to be the radius of the magnetic axis. Thus,

$$\psi_0=\int_0^{r_0}B_z(r,0)2\pi r\,dr. \quad (5)$$

(3) The average B_z in the midplane $z=0$ between the geometric axis $r=0$ and the magnetic axis $r=r_0$ is defined as B_0 so that

$$B_0=\frac{\int_0^{r_0}B_z(r,0)2\pi r\,dr}{\int_0^{r_0}2\pi r\,dr}=\frac{\psi_0}{\pi r_0^2}. \quad (6)$$

(4) Lengths are normalized to r_0 so

$$\bar{r}=r/r_0,\quad \bar{z}=z/r_0. \quad (7)$$

(5) The nominal ratio of hydrodynamic pressure to poloidal magnetic pressure at $z=0$ is defined as

$$\beta=\frac{\mu_0 P_0}{B_0^2}. \quad (8)$$

Strictly speaking, this defines the poloidal β, but since the toroidal and poloidal magnetic field energies in a spheromak are comparable, the poloidal and toroidal β's will be comparable (the total toroidal and poloidal field energies are exactly equal for a spheromak if $\beta=0$). All numerical β values specified in the remainder of this paper are the poloidal β defined by Eq. (8). Thus $\beta=1$ means that the poloidal field energy is approximately equal to the thermal energy; the qualification ''approximate'' is used here because B_0 is a nominal poloidal field magnitude and P_0 is the peak pressure.

(6) Both λ and ψ are written in nondimensional form as

$$\bar{\lambda}=\lambda r_0,\qquad \bar{\psi}=\psi/\psi_0. \quad (9)$$

Using these definitions and Eq. (4) the Grad–Shafranov equation becomes

$$\bar{r}\frac{\partial}{\partial\bar{r}}\left(\frac{1}{\bar{r}}\frac{\partial\bar{\psi}}{\partial\bar{r}}\right)+\frac{\partial^2\bar{\psi}}{\partial\bar{z}^2}+4\beta\bar{r}^2+\bar{\lambda}^2\bar{\psi}=0. \quad (10)$$

We now define

$$\chi=\bar{\psi}+4\frac{\beta}{\bar{\lambda}^2}\bar{r}^2, \quad (11)$$

so that the inhomogeneous Grad–Shafranov equation, Eq. (10), becomes the homogeneous equation

$$\bar{r}\frac{\partial}{\partial\bar{r}}\left(\frac{1}{\bar{r}}\frac{\partial\chi}{\partial\bar{r}}\right)+\frac{\partial^2\chi}{\partial\bar{z}^2}+\bar{\lambda}^2\chi=0. \quad (12)$$

Thus, χ satisfies a Helmholtz-type equation which has an infinite set of solutions. Since $\bar{\psi}$ must be an even function of $\bar{z}$ we attempt a solution of the form,

$$\chi=\bar{r}g(\bar{r})\cos\bar{k}\bar{z}, \quad (13)$$

where $\bar{k}$ is an arbitrary wave number and would correspond to an un-normalized wave number $k=\bar{k}/r_0$. Using this assumption Eq. (12) becomes

$$\bar{r}\frac{d}{d\bar{r}}\left(\frac{1}{\bar{r}}\frac{d}{d\bar{r}}\bar{r}g(\bar{r})\right)-\bar{k}^2\bar{r}g(\bar{r})+\bar{\lambda}^2\bar{r}g(\bar{r})=0, \tag{14}$$

which reduces to

$$\frac{d^2g}{d\bar{r}^2}+\frac{1}{\bar{r}}\frac{dg}{d\bar{r}}+\left(\bar{\lambda}^2-k^2-\frac{1}{\bar{r}^2}\right)g=0. \tag{15}$$

Equation (15) has the solutions $g=\sigma J_1(\sqrt{\bar{\lambda}^2-\bar{k}^2}\bar{r})$ if $\bar{\lambda}>\bar{k}$ and $g=\sigma I_1(\sqrt{\bar{k}^2-\bar{\lambda}^2}\bar{r})$ if $\bar{\lambda}<\bar{k}$, where σ is a constant to be determined. Since we are interested in solutions having a local maximum for ψ, we choose the solution involving J_1 (solutions involving I_1 are relevant to solar coronal loops and are described elsewhere[20]). The relevant solution to the Grad–Shafranov equation is therefore,

$$\bar{\psi}(\bar{r},\bar{z})=\sigma\bar{r}J_1(\bar{\gamma}\bar{r})\cos\bar{k}\bar{z}-4\frac{\beta}{\bar{\lambda}^2}\bar{r}^2, \tag{16}$$

where $\bar{\gamma}=\sqrt{\bar{\lambda}^2-\bar{k}^2}$. We also have the boundary condition that $\bar{\psi}(\bar{r},\bar{z})=1$ at $\bar{r}=1$, $\bar{z}=0$ so

$$1=\sigma J_1(\bar{\gamma})-4\frac{\beta}{\bar{\lambda}^2}. \tag{17}$$

This can be solved to determine σ, i.e.,

$$\sigma=\frac{1+4\dfrac{\beta}{\bar{\lambda}^2}}{J_1(\bar{\gamma})}. \tag{18}$$

Thus, the finite β spheromak has the poloidal flux function,

$$\bar{\psi}(\bar{r},\bar{z})=\left(1+4\frac{\beta}{\bar{\lambda}^2}\right)\bar{r}\frac{J_1(\bar{\gamma}\bar{r})}{J_1(\bar{\gamma})}\cos\bar{k}\bar{z}-4\frac{\beta}{\bar{\lambda}^2}\bar{r}^2. \tag{19}$$

The solution in the original (i.e., dimensioned) coordinates is

$$\frac{\psi(r,z)}{\psi_0}=\left(1+\frac{4\beta}{\lambda^2r_0^2}\right)\frac{r}{r_0}\frac{J_1(\gamma r)}{J_1(\gamma r_0)}\cos kz-\frac{4\beta r^2}{\lambda^2r_0^4}, \tag{20}$$

where $\gamma=\sqrt{\lambda^2-k^2}$. The force-free spheromak solution consists of setting $\beta=0$.

The magnetic axis is located at the maximum of $\psi(r,z)$. This position has coordinates $z=0$, $r=r_0$ and is the radial location where $\partial\psi/\partial r=0$. Thus, r_0 is the solution of

$$\left(1+\frac{4\beta}{\lambda^2r_0^2}\right)\frac{d}{dr}\left(\frac{r}{r_0}\frac{J_1(\gamma r)}{J_1(\gamma r_0)}\right)-\frac{8\beta}{\lambda^2r_0^3}=0. \tag{21}$$

Using the Bessel identities,

$$\frac{d}{ds}(sJ_1(s))=sJ_0(s), \tag{22}$$

$$sJ_2(s)=2J_1(s)-sJ_0(s), \tag{23}$$

Eq. (21) can be solved for β to give

$$\beta=\frac{\lambda^2r_0^2}{4}\frac{J_0(\gamma r_0)}{J_2(\gamma r_0)}. \tag{24}$$

As expected, setting $\beta=0$ constrains the magnetic axis for force-free equilibria to be at $r_0=x_{01}/\gamma$ where x_{01} is the first root of J_0.

Equation (24) shows that β is not an independent variable but instead is a function of $\lambda r_0=\sqrt{(kr_0)^2+(\gamma r_0)^2}$ and of γr_0. The constraint given by Eq. (24) forces $\psi(r,z)=\psi_0$ to be the maximum of ψ; without this constraint Eq. (20) would give $\psi(r,z)=\psi_0$, when $r=r_0$ and $z=0$ but $\psi(r,z)$ would not necessarily be a maximum at this location.

Substituting for β back into Eq. (20) gives

$$\frac{\psi(r,z)}{\psi_0}=\left(1+\frac{J_0(\gamma r_0)}{J_2(\gamma r_0)}\right)\frac{r}{r_0}\frac{J_1(\gamma r)}{J_1(\gamma r_0)}\cos kz-\frac{J_0(\gamma r_0)}{J_2(\gamma r_0)}\frac{r^2}{r_0^2}, \tag{25}$$

which now satisfies the constraints that $\psi(r_0,0)=1$ and also that $r=r_0$, $z=0$ is the location of the maximum value of ψ.

V. GEOMETRIC PROPERTIES OF THE FINITE β SOLUTION

A. Outer radius, height, and profile of the minor cross section

The radial outer boundary of the spheromak is at $z=0$ and the radial location where ψ vanishes. If we define this outer radius as $r=a$ then, using identity Eq. (23), the condition $\psi(a,0)=0$ becomes

$$2J_1(\gamma a)=J_0(\gamma r_0)\gamma a \tag{26}$$

which gives γa as a transcendental function of γr_0.

The $\beta=0$ equilibrium corresponds to solving Eq. (26) by setting $\gamma r_0=x_{01}$ and $\gamma a=x_{11}$ so that the right- and left-hand sides in Eq. (26) are each zero. For the more general case of finite β, Eq. (26) can be solved for γa in terms of γr_0 and so give a/r_0, the ratio of the outer radius to the radius of the magnetic axis. In addition, there are the constraints that $a>r_0$ and that β must be non-negative. Figure 1 plots a/r_0 and shows that a/r_0 decreases as γr_0 decreases below x_{01}, the force-free value. The point at the upper right corner on this finite length curve is $\gamma r_0=x_{01}=2.405$ and $a/r_0=x_{11}/x_{01}=1.593$, the $\beta=0$, force-free limit. Since β increases as γr_0 decreases, the decrease of a/r_0 as γr_0 decreases corresponds to Shafranov shift of the magnetic axis (i.e., an outwards shift with increasing β).

The profile of the spheromak boundary is given by

$$z=\frac{1}{k}\cos^{-1}\left(\frac{\gamma rJ_0(\gamma r_0)}{2J_1(\gamma r)}\right), \tag{27}$$

where r varies from 0 to a. For very small r, $J_1(\gamma r_0)\simeq\gamma r/2$ and so the normalized height of the geometric axis is

$$\frac{h}{r_0}=\frac{2}{kr_0}\cos^{-1}(J_0(\gamma r_0)). \tag{28}$$

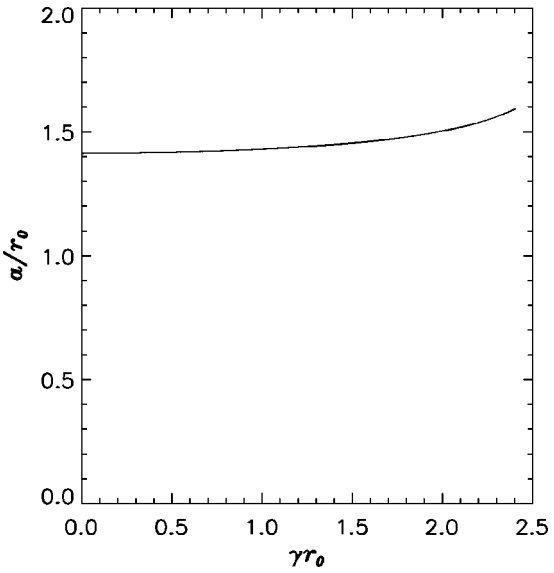

FIG. 1. Normalized outer radius a/r_0 vs γr_0.

In the force-free limit where $J_0(\gamma r_0)=0$, we obtain the usual quantization relation $k=\pi/h$, but for finite β equilibria, the relationship becomes $kh=2\cos^{-1}(J_0(\gamma r_0))$.

B. Safety factor

Since $\mu_0 I=\lambda\psi$ and $\psi\simeq B_z\pi r^2$ near the geometric axis, the trajectory of a field line near the magnetic axis is given by $d\phi/dz=B_\phi/rB_z=\lambda/2$ and so the increment in toroidal angle for a field line going up near the geometric axis is $\Delta\phi=\lambda h/2$. Thus, the number of toroidal turns per poloidal turn at the wall is

$$q_{\text{wall}}=\frac{\lambda}{2\pi k}\cos^{-1}(J_0(\gamma r_0)). \tag{29}$$

The safety factor on the magnetic axis is[14]

$$q_{\text{axis}}=\frac{\varepsilon^{1/2}+\varepsilon^{-1/2}}{\lambda r_0}, \tag{30}$$

where

$$\varepsilon=\left(\frac{\psi_{rr}}{\psi_{zz}}\right)_{r=r_0,z=0} \tag{31}$$

is a measure of the ellipticity of the poloidal flux surfaces near the magnetic axis. Straightforward calculation and application of Bessel identity Eq. (23) shows that

$$\varepsilon=\left(\frac{\gamma r_0}{kr_0}\right)^2, \tag{32}$$

so that

$$q_{\text{axis}}=\frac{1}{\gamma r_0}\frac{\lambda}{k}. \tag{33}$$

This is formally the same as the $\beta=0$ result but now γr_0 can be smaller than x_{01}. Thus q_{axis} can be much larger for finite β than for $\beta=0$.

The ratio of the safety factor on the magnetic axis to its value at the wall is

$$\frac{q_{\text{axis}}}{q_{\text{wall}}}=\frac{2\pi}{\gamma r_0\cos^{-1}(J_0(\gamma r_0))}, \tag{34}$$

which is independent of k and increases when γr_0 decreases; this is an approximate measure of the shear of the magnetic field.

Since β, q_{axis}, and q_{wall} are all functions of γr_0 and kr_0, these quantities can be compared by making contours in the positive quadrant of the γr_0, kr_0 plane with γr_0 restricted to be no larger than $x_{01}=2.405$ so that β is non-negative.

These analytic solutions should be useful for extending interchange stability calculations[21–23] of spheromaks to finite β and also for suggesting optimum wall shapes. Figure 2 gives plots of q_{wall}, q_{axis}, β, and h/r_0 as functions of γr_0 and kr_0; the locus of solutions with $\gamma r_0=x_{01}=2.405$ are the $\beta=0$, force-free solutions. Figure 3 plots $q_{\text{axis}}/q_{\text{wall}}$ as a function of γr_0. Figure 4 plots poloidal flux contours for several different choices of γr_0 and kr_0; these plots are arranged to correspond to the axes of Fig. 2. The right-hand column of plots in Fig. 4 consists of the $\gamma r_0=x_{01}=2.405$ force-free, $\beta=0$ solutions. Figure 4 shows that as the outermost flux profile becomes more rounded and then more triangular, a higher β results. Furthermore, by making γr_0 small, the spheromak becomes more oblate and so should be more immune to tilt instability. The solutions in Fig. 4 show that it is possible to have quite a range of shear profiles and β values and that some of these solutions have $q<1$ everywhere while others have $q>1$ on the magnetic axis and $q\ll 1$ at the wall.

These solutions indicate that if γr_0 is significantly less than $x_{01}=2.405$ and if the boundary has an appropriate profile, it is possible to have a very large poloidal β and a strong reversed shear (i.e., $q_{\text{axis}}\gg q_{\text{wall}}$). These features are of considerable interest because recent tokamak studies[24,25] have shown that reversed shear has desirable stabilizing properties and allows operation at much higher β than conventional shear (i.e., where $q_{\text{axis}}<q_{\text{wall}}$). The region of shear reversal in reversed shear tokamaks is localized to a core region surrounding the magnetic axis and this localized region improves the overall performance substantially. The finite β spheromak equilibria presented here have reversed shear everywhere and so the entire plasma corresponds to the beneficial core region of a reversed shear tokamak. The noncircularity appropriate for the reversed-shear equilibrium is prescribed by Eq. (25). Spheromaks differ from tokamaks because the toroidal field vanishes at the wall of a spheromak, whereas the toroidal field is finite at the wall of a tokamak and is essentially the vacuum toroidal field produced by the coils. Thus, q must eventually increase as the wall is approached in a tokamak. In contrast, q decreases in a spheromak as the wall is approached because the toroidal field goes to zero in which case the only contributor to q_{wall} is the helicity of the wall field lines as they circle the geometric axis.

Because the usual direct current (dc) helicity injection method used for creating and sustaining spheromaks tends to

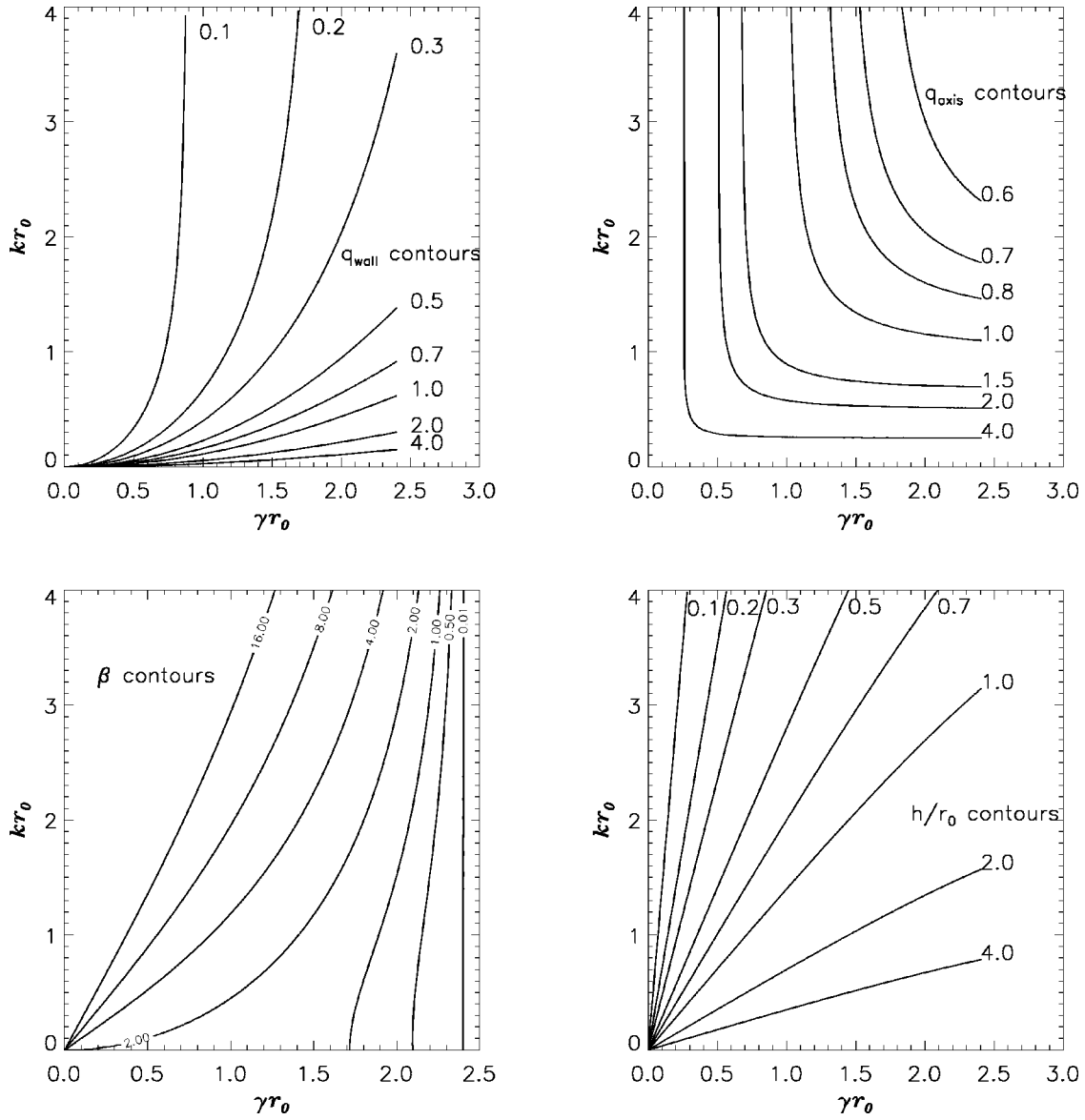

FIG. 2. Plots of q_{wall}, q_{axis}, β, and h/r_0 as functions of γr_0 and kr_0 using Eqs. (29), (33), (24), and (28), respectively. The horizontal coordinate $\gamma r_0 = x_{01} = 2.405$ corresponds to the force-free $\beta = 0$ cylindrical spheromak.

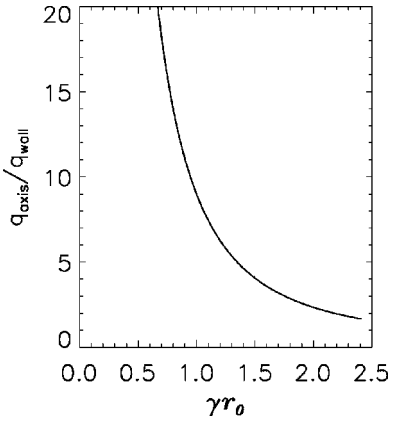

FIG. 3. Plot of shear $q_{\text{axis}}/q_{\text{wall}}$ as a function of γr_0. Shear increases as γr_0 decreases below $x_{01} = 2.405$, the force-force free value.

disrupt flux surfaces, it would probably be optimal to use dc helicity injection to form a low β seed spheromak and then build up the current and β of this seed spheromak using radio frequency (rf) current drive and/or neutral beam injection since these latter two methods do not disrupt flux surfaces.

Although the β used here is the poloidal β and not the β measured with respect to the total magnetic field, it is actually a reasonable figure of merit because the toroidal field in spheromaks is produced solely by plasma currents and so does not represent a direct capital cost. The poloidal field on the other hand is of the order of the toroidal currents in the flux conserving wall and so, if the wall is replaced by a set of equilibrium coils with toroidal currents, the poloidal β is a measure of how much plasma pressure is obtained for a given financial investment in these equilibrium coils.

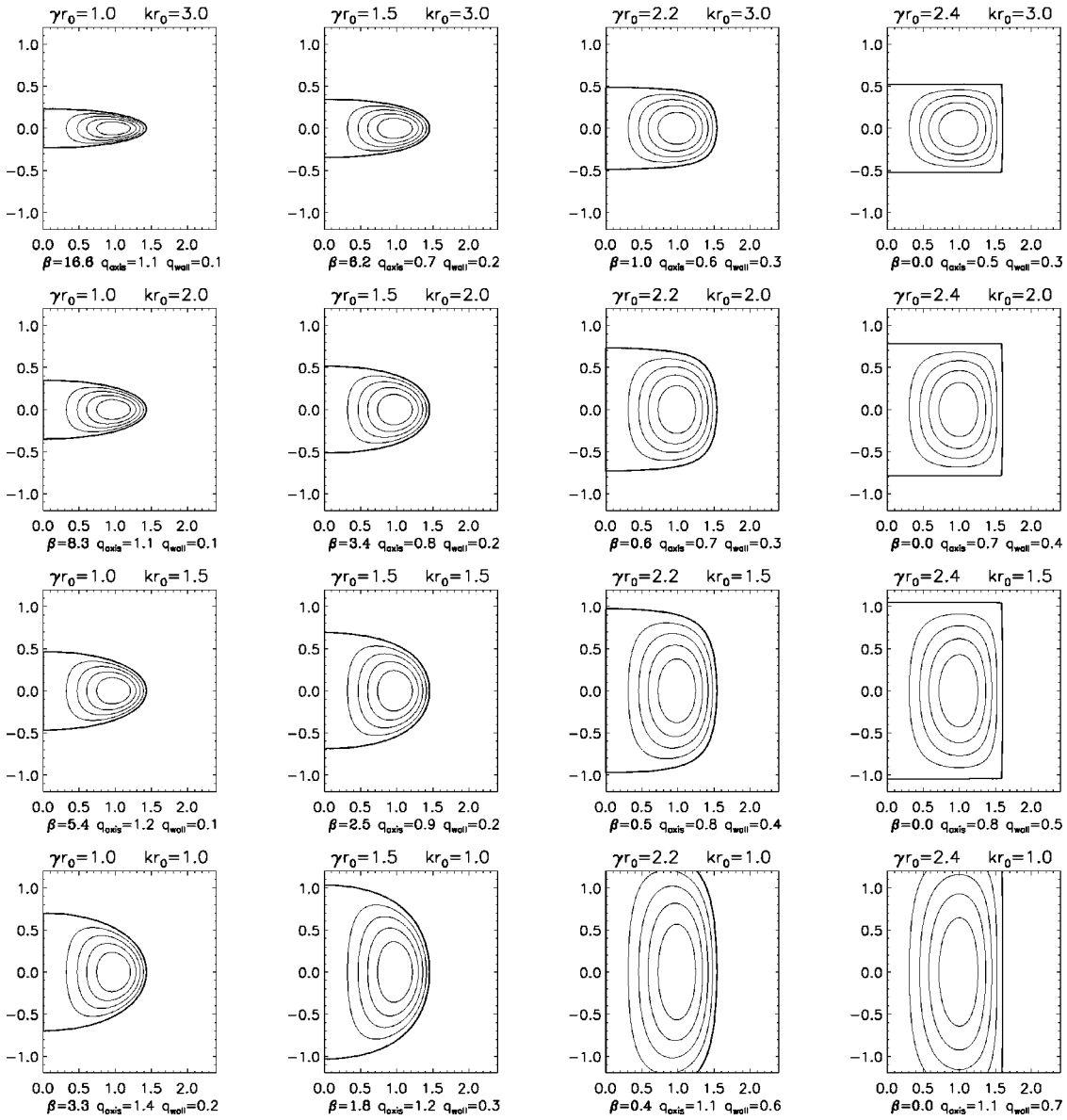

FIG. 4. Poloidal flux functions for the various choices of γr_0 and kr_0 indicated above each individual plot. The set of plots are arranged so as to correspond to the axes of Fig. 2 and the $\psi(r,z)/\psi_0=0.0$, 0.2, 0.4, 0.6, and 0.8 surfaces are drawn where the outermost surface is the $\psi(r,z)=0$ surface. The horizontal and vertical coordinates are in units of r_0 so that the magnetic axis is at the point (1,0). These contours can also be considered as surfaces of constant P/P_0 or I/I_0, where P_0 and I_0 are the respective maxima of P and I. The corresponding β, q_{axis}, and q_{wall} are shown below each plot. In order for the majority of the plots to be large enough to be legible, the third and fourth plots in the bottom row have been allowed to exceed the plotting area; these two equilibria are of lesser interest since their height is so large as to render them tilt unstable. The right hand column of plots have $\gamma r_0=x_{01}=2.405$ and are the cylindrical force-free $\beta=0$ equilibria.

VI. SUMMARY AND CONCLUSIONS

A finite β extension of the well-known cylindrical spheromak equilibrium has been derived and all relevant quantities have been shown to be functions of γr_0 and kr_0. This analytic solution suggests that it would be desirable to use flux conservers having the shape prescribed by Eq. (27) rather than a simple cylinder or sphere. The q profiles associated with these noncylindrical, noncircular shapes have strong reversed shear similar to what has been demonstrated to be beneficial for tokamaks and so these finite β spheromak equilibria may have good stability properties against pressure driven modes. Further investigations will be necessary to determine the detailed stability properties of these finite β equilibria, but the existence of a wide choice of poloidal β values, of shear values, of q ranges, and of shape profiles suggests at least a possibility for stable finite β equilibria. It should be noted that absolute MHD stability might not be strictly necessary because, as has been observed in both tokamaks and field reversed theta pinches, various non-MHD effects such as sheared velocity profiles, finite Larmor radius effects, and nonlinear saturation of instabilities can prevent an instability from becoming catastrophic.

ACKNOWLEDGMENT

Work supported by United States Department of Energy Grant No. DE-FG03-98ER54461.

[1]M. N. Rosenbluth and M. N. Bussac, Nucl. Fusion **19**, 489 (1979).
[2]H. P. Furth, Nucl. Instrum. Methods Phys. Res. **207**, 93 (1983).
[3]J. B. Taylor, Phys. Rev. Lett. **33**, 1139 (1974).
[4]T. R. Jarboe, Plasma Phys. Controlled Fusion **36**, 945 (1994).
[5]P. M. Bellan, *Spheromaks* (Imperial College Press, London, 2000).
[6]S. E. Gibson and B. C. Low, J. Geophys. Res. **105**, 18187 (2000).
[7]S. C. Hsu and P. M. Bellan, Mon. Not. R. Astron. Soc. (to be published).
[8]S. Chandrasekhar and P. C. Kendall, Astrophys. J. **126**, 457 (1957).
[9]W. C. Turner, E. H. A. Granneman, C. W. Hartman, D. S. Prono, J. Taska, and A. C. Smith, Jr., J. Appl. Phys. **52**, 175 (1981).
[10]E. M. Freire and R. A. Clemente, Plasma Phys. Controlled Fusion **27**, 389 (1985).
[11]E. K. Maschke, Plasma Phys. **15**, 535 (1973).
[12]F. Hernegger, in *Proceedings, 5th European Conference on Controlled Fusion and Plasma Physics, Grenoble, 1972* (Euratom-CEA, Paris, 1972), Vol. 1, p. 26.
[13]G. N. Throumoulopoulos and G. Pantis, Phys. Lett. A **121**, 423 (1987).
[14]J. M. Finn, W. M. Manheimer, and E. Ott, Phys. Fluids **24**, 1336 (1981).
[15]A. Bondeson, G. Marklin, Z. G. An, H. H. Chen, Y. C. Lee, and C. S. Liu, Phys. Fluids **24**, 1682 (1981).
[16]F. J. Wysocki, J. C. Fernandez, I. Henins, T. R. Jarboe, and G. J. Marklin, Phys. Rev. Lett. **65**, 40 (1990).
[17]H. Grad, Phys. Fluids **10**, 137 (1967).
[18]V. D. Shafranov, Rev. Plasma Phys. **2**, 103 (1966).
[19]H. R. Lewis and P. M. Bellan, J. Math. Phys. **31**, 2592 (1990).
[20]P. M. Bellan, Astrophys. J. (submitted).
[21]G. W. Hart, C. Chin-Fatt, A. W. DeSilva, G. C. Goldenbaum, R. Hess, and R. S. Shaw, Phys. Rev. Lett. **51**, 1558 (1983).
[22]R. M. Mayo and G. J. Marklin, Phys. Fluids **31**, 1812 (1988).
[23]U. Shumlak and T. R. Jarboe, Phys. Plasmas **7**, 2959 (2000).
[24]J. Manickam, M. S. Chance, S. C. Jardin, C. Kessel, D. Monticello, N. Pomphrey, A. Reiman, C. Wang, and L. E. Zakharov, Phys. Plasmas **1**, 1601 (1994).
[25]F. M. Levinton, M. C. Zarnstorff, S. H. Batha, M. Bell, R. E. Bell, R. V. Budny, C. Bush, Z. Chang, E. Fredrickson, A. Janos, J. Manickam, A. Ramsey, S. A. Sabbagh, G. L. Schmidt, E. J. Synakowski, and G. Taylor, Phys. Rev. Lett. **75**, 4417 (1995).